Progress In Electromagnetics Research, PIER 102, 213–226, 2010

MULTIBAND FOLDED LOOP ANTENNA FOR SMART PHONES

C.-W. Chiu and C.-H. Chang

Department of Electronic Engineering
National Ilan University
Ilan 260, Taiwan

Y.-J. Chi

Department of Electrical Engineering
National Chiao-Tung University
Hsinchu 350, Taiwan

Abstract—This paper presents a multiband folded loop antenna for smart phone applications. The proposed antenna with a symmetric loop pattern generates four resonance modes in the design bands. The current distributions of the excited resonance modes are analyzed to confirm the mode characteristic. Using a pair of tuning elements near the feed port, the impedance bandwidth is broadened to cover GSM850/GSM900/DCS/PCS/UMTS bands. This research performed simulation by a high frequency structure simulator (HFSS) to optimally design the antenna, and a practical structure was constructed to test. The current study measured the antenna parameters including reflection coefficient, radiation characteristics, peak gain, and radiation efficiency to validate the proposed antenna.

1. INTRODUCTION

The demand for multisystem handset equipment has recently increased rapidly. The design of a wireless transceiver in a smart phone or a portable device must support multisystem operations. Currently, multiband operation is almost a common standard. Therefore, the antenna embedded in the mobile phone or smart phone must be capable of operating at four or more frequency bands, at least including

Corresponding author: C.-W. Chiu (alexchiu@niu.edu).

GSM850/900 (824–960 MHz), DCS (1710–1880 MHz), PCS (1850–1990 MHz), UMTS (1920–2170 MHz). Moreover, internal antennas must have small size, weight, a low profile and as low cost as possible.

Much effort has been devoted to the multiband internal antenna during the past decade, such as planar inverted-F antennas (PIFA), inverted-F antennas (IFA), patch antennas and loop antennas [1]. The conventional PIFA, IFA, and their variants have become popular in most handsets and portable devices for mobile phone applications. This is mainly due to their miniature size, easy fabrication, and low cost [2, 3]. To achieve a wide bandwidth in the GSM850/900 band, the system ground plane of a PIFA or IFA acts as part of the antenna, thereby improving the bandwidth and gain performance [4–9]. This is necessary, especially as the mobile device is quite small. However, the current variation due to the device being hand-held and the resulting body proximity effect degrades antenna performance since the resonating currents are spread out over the system ground plane [1, 10]. To avoid degrading antenna performance, a printed loop antenna is another candidate for the mobile phone since the current induced on the ground plane is small [11–17].

This paper presents a folded loop antenna with multiband characteristics for smart phone applications. The proposed antenna is mounted on a printed circuit board. The proposed design applies a pair of rectangular tuning elements near the feed port to adjust resonance modes to cover the mentioned standards: GSM850/GSM900/DCS/PCS/UMTS. The occupied space of the folded loop antenna measures 60 mm$\times$ 10 mm $\times$8 mm. The main current is limited in the closed loop pattern and feed port area so that the current on the ground plane is small. Radiation degradation from the antenna system is reduced as the human head and hand are in the vicinity [15]. Details of the proposed antenna as well as experimental results are shown below.

2. ANTENNA DESIGN

Figure 1(a) shows the three-dimensional configuration of the proposed antenna. The antenna is mounted on a 1.6-mm thick FR4 substrate with a relative permittivity of 4.4 and a loss tangent of 0.02. The metal pattern of the antenna consists of a folded loop strip and two tuning strip lines. Fig. 1(b) shows the size of the unfolded loop antenna. Total length of the folded loop strip from P_1 to P_2 is about 164 mm, close to one-half wavelength of the frequency 928 MHz. On the same side of the substrate, a ground plane of width 60 mm and length 100 mm is printed as the system ground plane of a mobile device, such as a

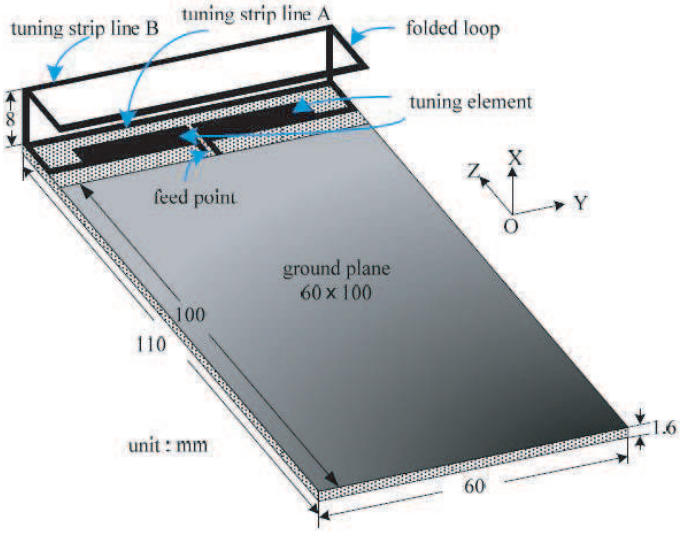

(a)

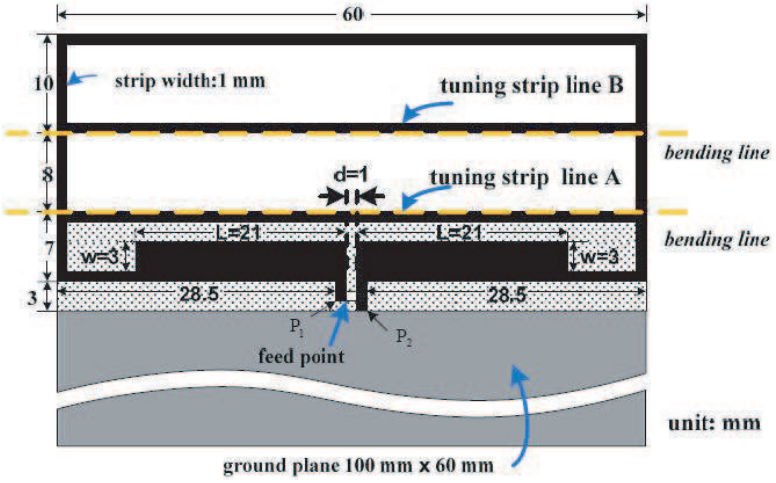

(b)

Figure 1. Geometry of the proposed antenna: (a) 3D View. (b) Plan view of the front-side.

smart phone. To increase electric length and support the folded loop, two tuning strip lines A and B are inserted into the loop. A pair of rectangular tuning elements is placed near the feed port to broaden the impedance bandwidth. The antenna is fed by a 50 ohm semi-grid

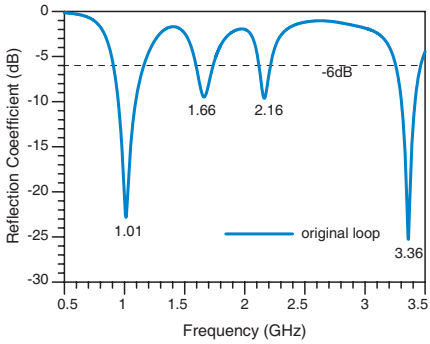

Figure 2. Simulated results of the reflection coefficient for the original loop pattern.

coaxial cable. The center conductor of the cable launches the signal from the left-side strip terminal P_1 at the feed point and the outer conductor of the cable is affixed to the right-side strip end P_2 which terminates to the ground plane.

The antenna system has a symmetric loop pattern but an unbalanced feeding scheme. The antenna system generates four resonance modes below 3.5 GHz. Even modes and odd modes can be simultaneously excited on this antenna system. Fig. 2 shows simulation results for the reflection coefficient without the tuning element and the tuning strip lines by Ansoft's HFSS, an EM simulator. The first resonance at 1.01 GHz is an even mode (one-half wavelength mode) and the third resonance at 2.16 GHz is its higher mode. The second resonance at 1.66 GHz is an odd mode (one-wavelength mode) and the fourth resonance at 3.36 GHz is its higher order mode [17].

Surface current distributions on the conductor strip confirm the mode characteristic. Fig. 3 shows the vector surface current distributions and current densities on the loop pattern at the four resonance frequencies 1.01, 1.66, 2.16 and 3.36 GHz, respectively. The current distributions shown in Figs. 3(a) and (c) are equal in magnitude but in the opposite direction since the loop pattern is symmetric from the side with respect to the line pp'. This behavior implies that the unbalanced feeding scheme excites the even modes. The current distribution shown in Fig. 3(c) has three nulls so that it is a 1.5-wavelength mode [15]. The currents shown in Figs. 3(b) and (d) show a differential behavior in the feed port. The currents are equal in amplitude and in the same direction respective to qq'. This behavior exhibits that they are odd modes. They are the traditional one- and two-wavelength loop modes [15]. The antenna at the second resonance

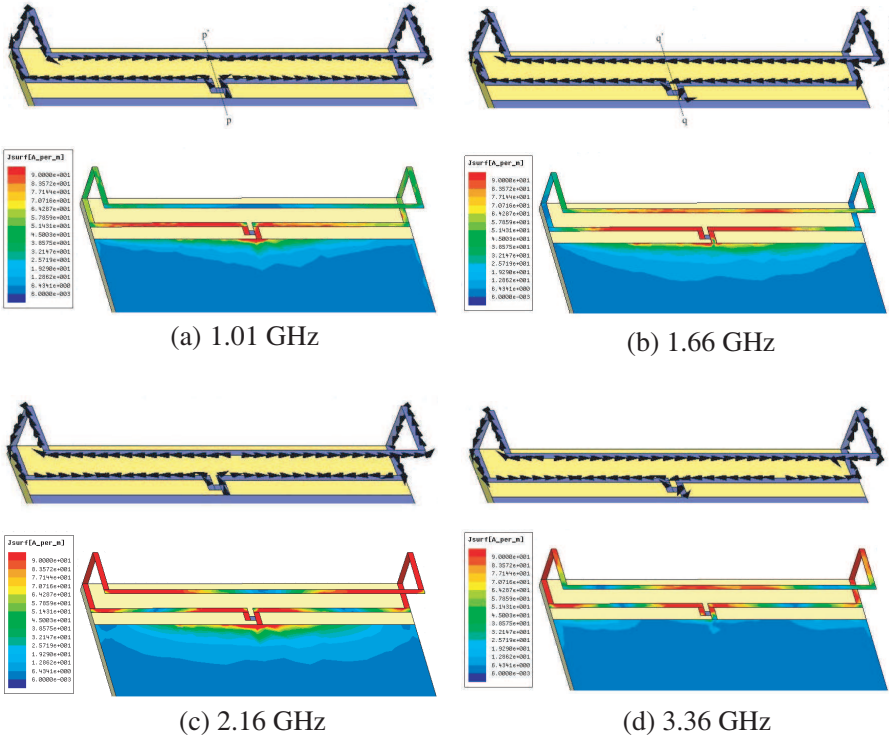

(a) 1.01 GHz (b) 1.66 GHz

(c) 2.16 GHz (d) 3.36 GHz

Figure 3. Simulated vector current distributions and surface current densities.

looks like a differential folded dipole since the currents at 1.66 GHz flow in the same direction for all the strips.

3. BANDWIDTH ENHANCEMENT

To cover the bandwidth for UMTS system application, some bandwidth enhancement techniques must be applied to broaden the impedance bandwidth in the higher band. The folded antenna is a three-dimensional structure where the strip width is only 1 mm so that it must have a solid support. To stably support the 3-D antenna, two tuning strip lines A and B are inserted into the loop and bent at the upper and lower folding corners, as shown in Figs. 1(a) and (b). The main purpose of inserting the tuning strip lines is to increase the electrical length of resonant frequency at the lower band. Fig. 4 shows the influence of the strip lines A and B on the reflection coefficient. The

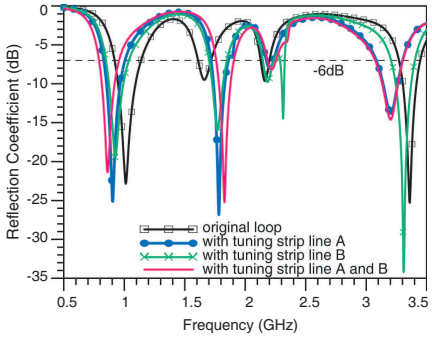

Figure 4. Frequency shifting down with inserted tuning strip lines.

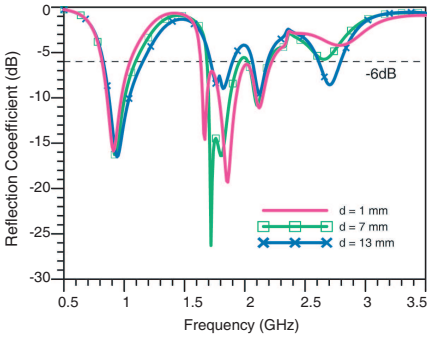

Figure 5. Simulated results as a function of the distance d between the pair of tuning elements.

finding shows that the first resonance frequency shifts from 1.01 GHz to 0.86 GHz. The electric length of the one-half wavelength increases since the input impedance is capacitive in the low band. However, resonant frequency of the one-wavelength differential mode shifts to higher frequencies because shunting an inductance in the loop pattern decreases the parallel inductance and then reduces total electrical length of the series-resonance loop mode. Adding the tuning strip line B generates a new resonance mode at the resonant frequency 2.3 GHz. The current distribution which has three nulls on the loop pattern is similar to the distribution shown in Fig. 3(c). The new mode is a 1.5-wavelength mode of the closed loop where the current flows through the tuning strip line B.

Although the folded antenna generates three resonance modes in the higher band, the achieved bandwidth is not wide enough to cover DCS, PCS, and UMTS bands. To obtain better impedance matching in the higher band, a pair of tuning elements shown in Fig. 1(b) is adhered to the loop strip near the feed port. Investigating the current distribution shown in Figs. 3(a) and (b) decides the tuning element position. Since the current is strong near the feed port, impedance matching is easier to achieve by placing the tuning element near this area. Varying the location d, width w and length L of the tuning element helps achieve impedance matching over the design bands. Fig. 5 shows the position influence of the tuning element on antenna performance when the distance d varies from 1 to 13 mm. The position tuning for the pair of tuning element is controlled by the distance d. The symmetric feature is preserved here and the length L and the width w are fixed. The finding shows that the position influence is larger in

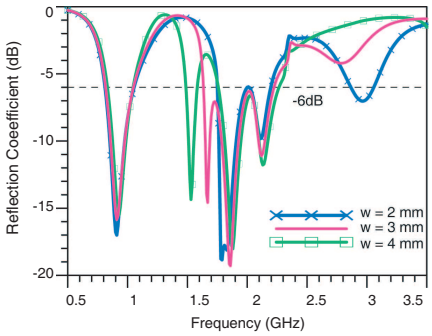

Figure 6. Simulated results as a function of width w of the tuning element.

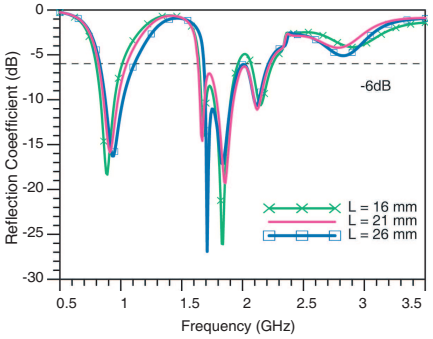

Figure 7. Simulated results as a function of length L of the tuning element.

the high band than in the low band. When the tuning element is located near the middle ($d = 1$ mm), impedance matching is good for covering GSM850/GSM900/DCS/PCS/UMTS operation.

This research also conducted a parametric study on the width w and the length L. When the parameter w varies from 2 to 4 mm or the parameter L varies from 16 to 26 mm, other dimensions of the antenna are the same as shown in Fig. 1. Fig. 6 shows the simulation reflection coefficient as a function of width w. The width variation does not influence impedance matching in the low band but findings show larger effects in the higher band. When the width w is fixed as 3 mm, the impedances are well matched in the higher band. Fig. 7 shows the effects of length L on antenna performance. Observations show larger effects on the first resonance mode. The longer the length, the greater the bandwidth. When the length is increased to about 21 mm, the bandwidths in the low band and higher band achieve the SWR < 3 bandwidth requirement.

The current work also studies the proposed antenna with different ground-plane lengths L_g. Fig. 8 shows simulated results for length L_g variations from 80 to 120. The finding shows that the bandwidth of the low band becomes broader when length L_g increases. Bandwidths in the low band for $L_g = 80$ mm and $L_g = 120$ mm are 160 MHz and 250 MHz, respectively. The bandwidth for $L_g = 80$ mm is still 72% of that for $L_g = 100$ mm. Center resonance frequency in the low band is slightly influenced by ground plane length. Traditional PIFA has a quarter-wavelength shorted patch and a finite ground plane [10]. The ground plane acts as part of a resonator in the lower band. Ground plane size has strong effect on impedance matching,

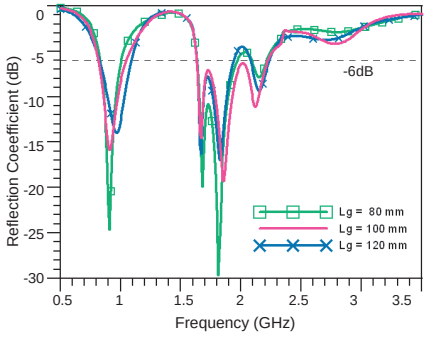

Figure 8. Simulated results as a function of length L_g (system ground plane length).

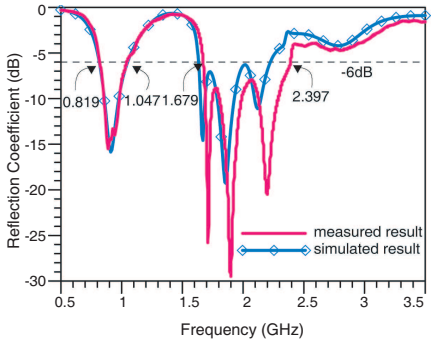

Figure 9. Measured results compared with simulation results.

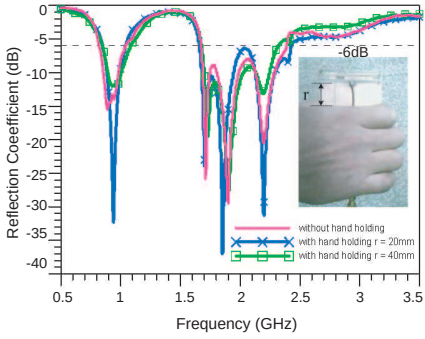

Figure 10. Measured results with and without hand holding.

resonance frequency and antenna gain performance. This result shows that a ground plane around 120 mm at GSM900 frequencies improves the bandwidth since it excites a ground plane mode. In some situations, 120 mm may be too large for a handset phone. Therefore some researchers propose to electrically enlarge the ground plane by adding slots on the ground plane [4–10]. As a result, handhold and head proximity degrade antenna performance.

4. RESULTS AND DISCUSSION

The proposed antenna shown in Fig. 1 has been constructed and tested. Measurements were taken using a network analyzer E5071B. Fig. 9 shows the measured reflection coefficient compared with the simulated results by HFSS. The results show good agreement except over 2 GHz.

Findings show some differences beyond 2 GHz because of some loss effect on the substrate. The bandwidth achieved with the reflection coefficient better than −6 dB is 228 MHz (0.819–1.047 GHz) in the lower band and 718 MHz (1.679–2.397 GHz) in the DCS/PCS/UMTS band. (The internal antenna for general mobile phone applications is typically designed based on the bandwidth definition of −6 dB reflection coefficient).

This work also studied the effects of user's hand-hold on the mobile phone with the proposed antenna [11, 18–21]. The distance r from the top edge of the ground plane to the top rim of the user's thumb portion is about 20 mm and 40 mm, respectively. Fig. 10 shows

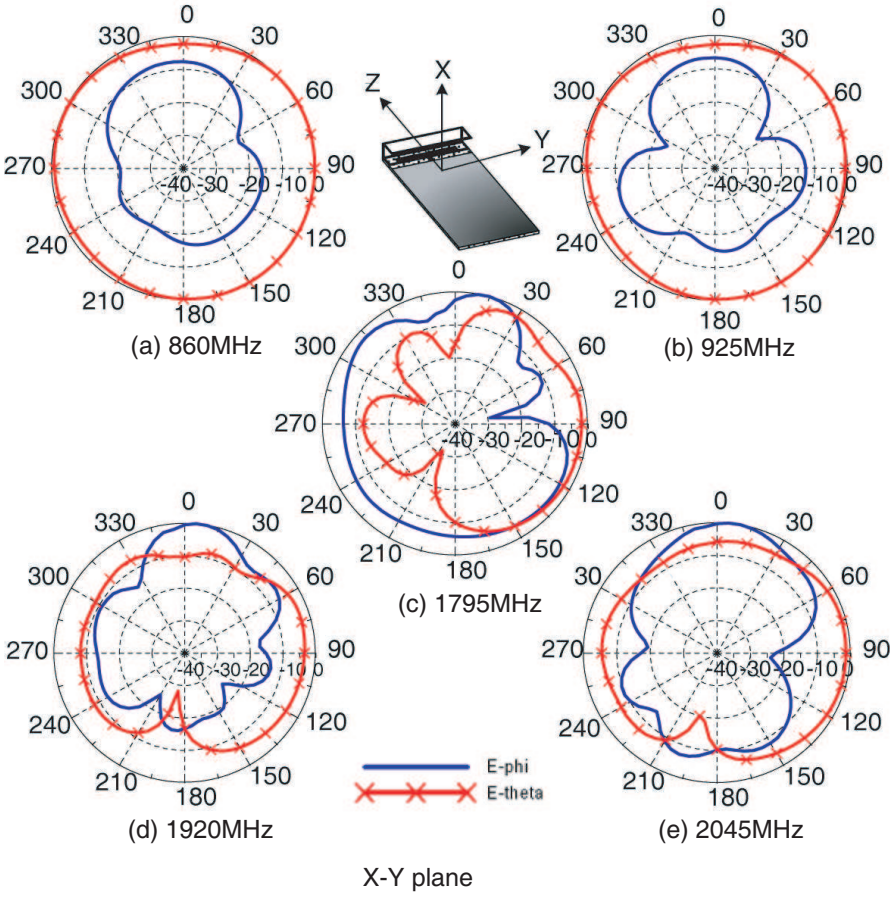

Figure 11. Measured radiation patterns at 860 MHz, 925 MHz, 1.795 GHz, 1.92 GHz, and 2.045 GHz, respectively.

the measured results when hand-holding the antenna. The figure also shows the measured results without hand-holding. The smaller frequency detuning indicates that loop antenna performance is less dependent on the ground plane. Since the proposed antenna has balance features and less currents on the ground plane, the handheld influence of the loop antenna on impedance matching is less than that of the planar inverted-F antenna.

The radiation-pattern and gain measurement were performed in the anechoic chamber of SGS Ltd., Taiwan. Fig. 11 plots the measured radiation patterns at 860 MHz, 925 MHz, 1.795 GHz, 1.92 GHz, and 2.045 GHz for the proposed antenna. At 925 MHz, the radiation pattern has a dipole-like feature. Findings show more variations for the radiation pattern in the higher band, since high order modes are generated in the higher band. A nearly omni-directional radiation pattern was found on the XY-plane. The feature is very suitable for mobile phones.

Figure 12 shows measured peak gains and radiation efficiencies. The peak gains and the efficiencies were measured directly from the SGS anechoic chamber using the ETS-Lindgren model AMS-8500 antenna measurement system and the 3164-08 open boundary quad-ridged horn antenna. The measured results of the gain also included the loss of a 120 mm mini-coaxial cable. The measured antenna gain over the GSM band varies from around 1.4–3.3 dBi and the radiation efficiency is larger than 70%. The measured antenna gain for the higher band varies around 2–5.5 dBi and the radiation efficiency is larger than 55%.

The specific absorption rate (SAR) of the proposed antenna is studied using the FEKO simulation software [22]. Fig. 13 shows

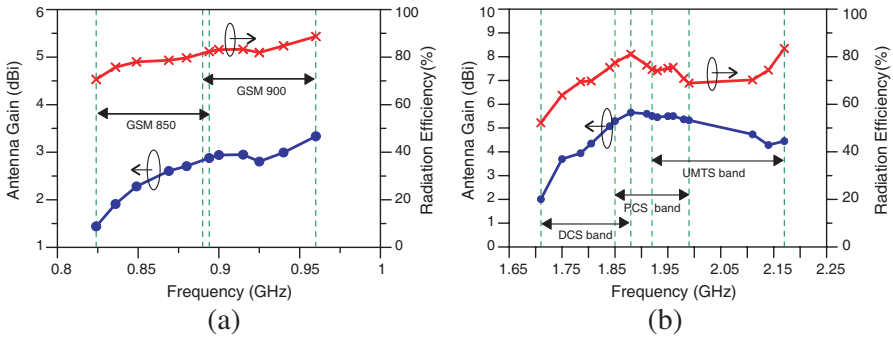

Figure 12. Measured peak gain and radiation efficiency, (a) in the low band and (b) in the higher band.

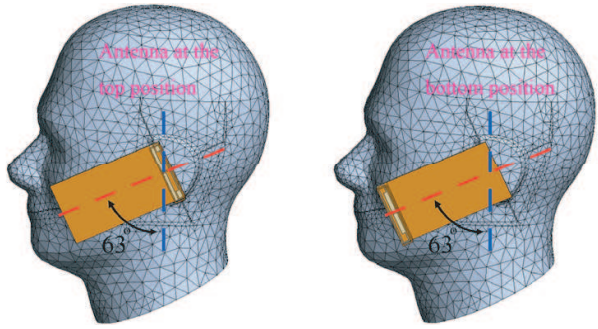

Figure 13. Simulation model with the proposed antenna for the SAR analysis.

Table 1. Simulated 1-g average SAR (W/kg) at GSM850/GSM900 /DCS/PCS/UMTS bands.

Band	GSM850	GSM900	DCS	PCS	UMTS
Frequency (MHz)	$f = 836.6$	$f = 914.8$	$f = 1747$	$f = 1880$	$f = 1950$
At the top (W/kg)	2.432	2.119	2.137	1.841	2.883
At the bottom	1.620	1.626	0.532	0.546	1.418

the simulation model with the antenna placed at the cheek position near the phantom. The separation distance between the system ground plane and the earpiece of the SAR phantom head is 5 mm. The tilted angle between the center line of the printed circuit board and the vertical line of the phantom is 63°. The antenna is placed at the top edge of the system ground plane or at the bottom position (rotating 180°). The testing power is 24 dBm (0.25 W) at GSM850/GSM900/UMTS bands; while the testing power is 20.8 dBm (0.121 W) at DCS/PCS bands [16]. Table 1 listed the simulated 1-g average SARs at the transmitting frequencies 836.6, 914.8, 1747, 1880, and 1950 MHz. The finding shows that the SAR at the bottom position is lower than at the top position owing to larger distance to the cheek. It seems that placing the antenna at the bottom edge is more promising for practical mobile phone applications.

5. CONCLUSION

This paper presented a folded loop antenna with five-band characteristics. Four resonance modes are excited on the symmetric loop pattern in the design band. The proposed antenna utilizes a pair of tuning elements coated on the printed circuit board to achieve wideband performance. The design parameters of the folded loop antenna are optimized using Ansoft's HFSS software and a practical structure is constructed to test. Measured parameters including reflection coefficient, radiation patterns, peak gain, and radiation efficiency are presented to validate the proposed design. The loop antenna is less dependent on the ground plane so that antenna performance is less influenced by hand-holding the device and head proximity. The structure is very suitable for portable device and can be readily integrated in a smart phone.

ACKNOWLEDGMENT

We are grateful to the National Center for High-performance Computing for the HFSS computer time and use of facilities. Also, the authors would like to thank Mr. Cheng-Chang Chen, Bureau of Standards, Metrology and Inspection, M.O.E.A, Taiwan, for his help in the SAR simulation using the FEKO simulation tool.

REFERENCES

1. Morishita, H., Y. Kim, and K. Fujimoto, "Design concept of antenna for small mobile terminals and the future perspective," *IEEE Transactions on Antennas and Propagation*, Vol. 55, No. 5, 30–43, Oct. 2002.
2. Chi, Y. J., C. W. Chiu, and S. M. Deng, "Internal quad-band printed antenna for PDA phone," *Electronics Letters*, Vol. 45, No. 10, 489–491, May 2009.
3. Chiu, C. W. and Y. J. Chi, "Planar hexa-band inverted-F antenna for mobile device applications," *IEEE Antenna and Wireless Propagation Letters*, Vol. 8, 1099–1102, 2009.
4. Hossa, R., A. Byndas, and M. E. Bialkowski, "Improvement of compact terminal antenna performance by incorporating open-end slots in ground plane," *IEEE Microwave and Wireless Component Letters,* Vol. 14, No. 6, 283–285, Jun. 2004.
5. Abedin, M. F. and M. Ali, "Modifying the ground plane and its effect on planar inverted-F antennas (PIFAs) for mobile phone

handsets," *IEEE Antennas and Wireless Propagation Letters*, Vol. 2, 226–229, 2003.

6. Anguera, J., I. Sanz, A. Sanz, A. Condes, D. Gala, C. Puente, and J. Soler, "Enhancing the performance of handset antennas by means of groundplane design," *IEEE International Workshop on Antenna Technology: Small Antennas and Novel Metamaterials (IWAT)*, 29–32, New York, USA, Mar. 2006.
7. Cabedo, A., J. Anguera, C. Picher, M. Ribó, and C. Puente, "Multi-band handset antenna combining PIFA, slots, and ground plane modes," *IEEE Transactions on Antennas and Propagation*, Vol. 57, No. 9, 2526–2533, Sep. 2009.
8. Picher, C., J. Anguera, A. Cabedo, C. Puente, and S. Kahng, "Multiband handset antenna using slots on the ground plane: Considerations to facilitate the integration of the feeding transmission line," *Progress In Electromagnetics Research C*, Vol. 7, 95–109, 2009.
9. Antonino, E., C. A. Suárez, M. Cabedo, and M. Ferrando, "Wideband antenna for mobile terminals based on the handset PCB Resonance," *Microwave and Optical Technology Letters*, Vol. 48, No. 7, 1408–1411, Jul. 2006.
10. Vainikainen, P., J. Ollikainen, O. Kivekas, and K. Kelander, "Resonator-based analysis of the combination of mobile handset antenna and chassis," *IEEE Transactions on Antennas and Propagation*, Vol. 50, No. 10, 1433–1444, Oct. 2002.
11. Morishita, H., H. Furuuchi, and K. Fujimoto, "Performance of balanced-fed antenna system for handsets in the vicinity of a human head or hand," *IEE Proceedings on Microwave, Antennas and Propagation*, Vol. 149, No. 2, 85–91, Apr. 2002.
12. Jung, B., H. Rhyu, Y. J. Lee, F. J. Harackiewwicz, M. J. Park, and B. Lee, "Internal folded loop antenna with tuning notches for GSM/GPS/DCS/PCS mobile handset applications," *Microwave and Optical Technology Letters*, Vol. 48, No. 8, 1501–1504, Aug. 2006.
13. Lin, C. I. and K. L. Wong, "Internal meandered loop antenna for GSM/DCS/PCS multiband operation in a mobile phone with the user's hand," *Microwave and Optical Technology Letters*, Vol. 49, No. 4, 759–765, Apr. 2007.
14. Chi, Y. W. and K. L. Wong, "Internal compact dual-band printed loop antenna for mobile phone application," *IEEE Transactions on Antennas and Propagation*, Vol. 55, No. 5, 1457–1462, May 2007.
15. Wong, K. L. and C. H. Huang, "Printed loop antenna with

a perpendicular feed for penta-band mobile phone application," *IEEE Transactions on Antennas and Propagation*, Vol. 56, No. 7, 2138–2141, Jul. 2008.

16. Chi, Y. W. and K. L. Wong, "Compact multiband folded loop chip antenna for small-size mobile phone," *IEEE Transactions on Antennas and Propagation*, Vol. 56, No. 12, 3797–3803, Dec. 2008.
17. Chi, Y. J. and C. W. Chiu, "An internal hepta-band printed loop antenna for laptop computer," *Proc. IEEE AP-S Int. Symp.*, Jun. 2009.
18. Boyle, K. R., Y. Yuan, and L. P. Lighthart, "Analysis of mobile phone antenna impedance variations with user proximity," *IEEE Transactions on Antennas and Propagation*, Vol. 55, No. 2, 364–372, Feb. 2007.
19. Huang, T. and K. R. Boyle, "User interaction studies on handset antennas," *The Second European Conference on Antennas and Propagation*, Nov. 2007.
20. Arenas, J. J., J. Anguera, and C. Puente, "Balanced and single-ended handset antennas: Free space and human loading comparison," *Microwave and Optical Technology Letters*, Vol. 51, No. 9, 2248–2254, Sep. 2009.
21. Anguera, J., A. Camps, A. Andúar, and C. Puente, "Enhancing the robustness of handset antennas to finger loading effects," *Electronics Letters*, Vol. 45, No. 15, 770–771, Jul. 2009.
22. FEKO, EM Software & Systems-S.A. (Pty) Ltd (EMSS) [Online]. Available: http://www.feko.info.